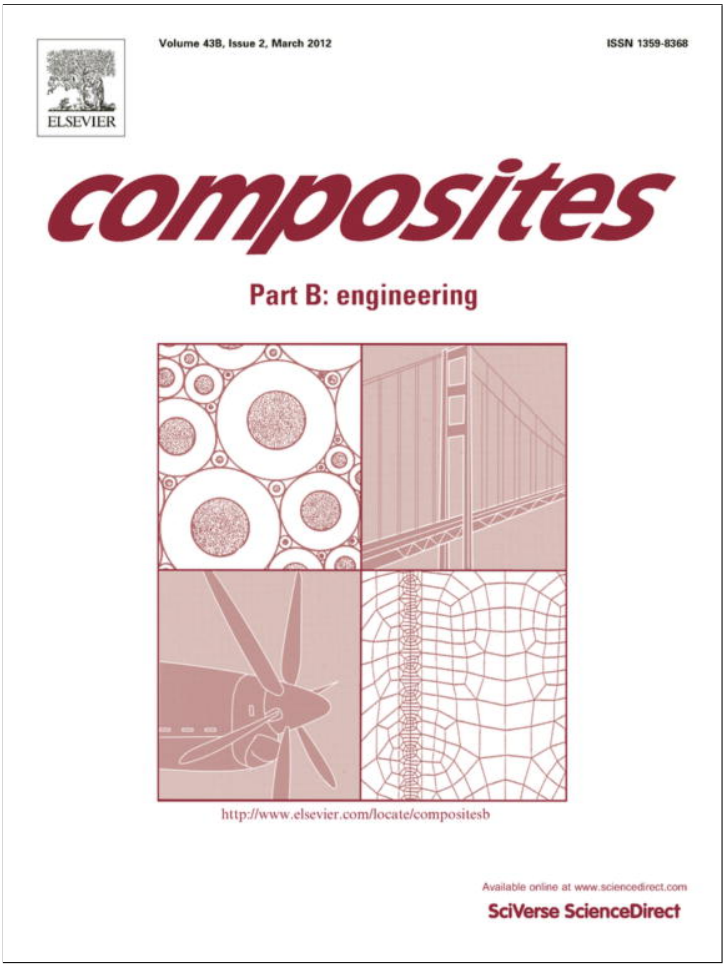

Composites: Part B 43 (2012) 228–239

Contents lists available at SciVerse ScienceDirect

Composites: Part B

journal homepage: www.elsevier.com/locate/compositesb

Prediction of strength parameters of FRP-confined concrete

H.M. Elsanadedy, Y.A. Al-Salloum, H. Abbas *, S.H. Alsayed

Specialty Units for Safety and Preservation of Structures, Department of Civil Engineering, King Saud University, Riyadh 11421, Saudi Arabia

ARTICLE INFO

Article history:
Received 19 March 2011
Received in revised form 15 June 2011
Accepted 22 August 2011
Available online 28 August 2011

Keywords:
A. Polymer-matrix composites (PMCs)
A. Fibres
B. Strength
C. Statistical properties/methods
Concrete

ABSTRACT

This research deals with the prediction of compressive strength and crushing strain of FRP-confined concrete using neural networks and regression models. Basic information on neural networks and the types of neural networks most suitable for the analysis of experimental results are given. A set of experimental data, covering a large range of parameters, for the training and testing of neural networks is used. The prediction models based on neural network are presented. The influence of raw and the non-dimensional group of variables on compressive strength and crushing strain of FRP-confined concrete is studied through sensitivity analysis, which provided a basis for the development of a new regression based model. The neural networks based model gave high prediction accuracy and the results demonstrated that the use of neural networks in assessing the compressive strength and crushing strain of FRP-confined concrete is both practical and beneficial.

1. Introduction

It is well established that external confinement of concrete cylinder (e.g. column) enhances its strength and ductility. Until the early 1990s, the external confinement was mainly provided by either constructing an additional reinforced concrete cage or installing grout-injected steel jackets. Steel jacketing is more effective than caging, because the latter results in a substantial increase in the cross-sectional area and self weight of the structure. Both methods are, however, labor intensive and sometimes difficult to implement on site. In addition to being heavy, steel jackets are also poor in resisting weather attacks. Nowadays, fiber reinforced polymers (FRPs) have started to be used as confining materials in structures and the technique of FRP strengthening of reinforced concrete columns has replaced conventional steel jacketing dramatically [1]. FRP has advantages such as: high strength-to-weight ratio, high confinement strength, easy to install and maintain, fatigue resistant, non-magnetic, non-metallic, and durable. FRP-wrapping, prefabricated sheet jacketing and filament winding can substantially enhance the axial compressive strength and ductility of concrete cylinders due to lateral confinement of FRP. A clear understanding of the strength and ductility of FRP-confined concrete is necessary for constructing a stress–strain model of FRP-confined concrete in order to evaluate overall strengthening effects of columns retrofitted by FRP composites.

In recent past, substantial work is reported on FRP-strengthened columns or concrete cylinders. These studies were mainly conducted on the compressive strength and stress–strain behavior of FRP-confined concrete [1–43]. Demers and Neale [2] investigated the effectiveness of FRP wrapping for strengthening of plain concrete cylinders. They wrapped cylinders through one and three layers of FRP. They observed increase in strength up to 70% and ductility up to seven times than that of unwrapped plain concrete cylinders. Toutanji and Balagurce [3] investigated effectiveness of FRP wrapping for strengthening plain concrete cylinders. Two layers of CFRP or GFRP wrap were applied to the cylinder. They observed 200% and 100% increase in the compressive strength with CFRP and GFRP wraps, respectively. The studies have shown that FRP-confined concrete behaves differently from steel-confined concrete [4], so design recommendations developed for steel-confined concrete columns (or cylinders) cannot be applied to FRP-confined columns despite the apparent similarity between these two types of columns or cylinders. Parvin and Jamwal [5] investigated the behavior of small-scale FRP-wrapped concrete cylinders under uniaxial compressive loading using non-linear finite element analysis. They considered two parameters for the numerical study: the FRP wrap thickness, and the ply configuration. The finite element analysis results showed substantial increase in the axial compressive strength and ductility of the FRP-confined concrete cylinders as compared to the unconfined ones. The increase in wrap thickness also resulted in enhancement of axial strength and ductility of the concrete cylinders. Berthet et al. [6] presented the results of an experimental investigation concerning the compressive behavior of short concrete columns externally confined by carbon and E-glass FRP jackets. The results showed that external confinement can significantly improve the ultimate strength and ductility of the specimens. Lam and Teng [7] proposed a design-oriented stress–strain model for concrete confined by FRP wraps

* Corresponding author.
E-mail address: abbas_husain@hotmail.com (H. Abbas).

1359-8368/$ - see front matter © 2011 Elsevier Ltd. All rights reserved.
doi:10.1016/j.compositesb.2011.08.043

with fibers only or predominantly in the hoop direction. The model is based on a careful interpretation of existing test data and observations. The predictions of the model were found to agree well with test data. Almusallam [8] conducted a comprehensive experimental program which involved 54 plain concrete cylinders with varying compressive strength wrapped with E-glass/epoxy fiber reinforced polymer (GFRP) jackets and subjected to uniaxial compressive loads. The influence of number of composite plies (i.e. composite thickness) and compressive strength of concrete on the behavior of the GFRP-confined cylinders was investigated. The results of this study showed that: (i) compressive strength and ductility of the concrete cylinders increases with number of composite layers; and (ii) effect of confinement is substantial for normal strength concrete and marginal for high-strength concrete. A semi-empirical theoretical model was also developed in order to predict stress–strain relationship of GFRP-confined concrete cylinders. The model results showed an excellent agreement with experimental values. Youssef et al. [9] developed a stress–strain model for concrete confined by fiber reinforced polymer (FRP) composites. The model was based on the results of a comprehensive experimental program including large-scale circular, square and rectangular short columns confined by carbon/epoxy and E-glass/epoxy jackets providing a wide range of confinement ratios. Ultimate stress, rupture strain, jacket parameters, and cross-sectional geometry were found to be significant factors affecting the stress–strain behavior of FRP-confined concrete. Such parameters were analyzed statistically based on the experimental data, and equations to theoretically predict these parameters were presented. Experimental results from this study were compared with the proposed semi-empirical model as well as others from the literature.

Although many studies have been carried out on FRP-confined concrete, there are still some issues worth being discussed further: (i) early models have been developed based on a limited test data that is one of the weakness of the existing models in which further applicability of their approaches could not be guaranteed; (ii) many models were derived from steel-confined concrete models, whereas extensive experimental results have shown that the stress–strain behavior of FRP-confined concrete cylinders is significantly different from that of steel-confined concrete; so they are often not effective enough; (iii) the ultimate rupture strain of FRP has a great influence on the behavior of FRP-confined concrete cylinders, which is seldom considered by the existing models; and (iv) few experiments and analyses were found to consider strength and ductility of FRP-confined concrete cylinders with strain-softening responses, although it is closer to the case of real structures.

Some investigators [44,45] have used the strain efficiency factor in the prediction of the compressive strength of FRP-confined concrete. The theoretical models used in these studies for the estimation of strain efficiency factor are based on many assumptions such as ignoring stress localization and bond/friction between FRP and concrete. Further, the change in diameter of concrete cylinders would also depend upon the Poisson's ratio of concrete whose value varies with the level of stress due to micro-cracking. The value of Poisson's ratio of concrete seems to have been taken as constant in the analysis. These models require some material parameters, such as Poisson's ratios of FRP material, which are not available in the literature. It is due to these reasons that the strain efficiency factor has not been considered in the analysis presented in this paper.

In recent years, artificial neural networks (ANNs) have been of interest to researchers in the modeling of various civil engineering systems. The FRP-confined concrete is affected by unknown multivariable interrelationships and the existing experimental data are noisy; consequently, the models derived by regression analysis are not able to predict the behavior well. The ANN automatically manages the relationships between variables and adapt based on the data used for their training. So, it is important to collect a large number of experimental data. In this study, a large test database built from an extensive survey of existing tests on FRP-confined circular concrete specimens is carefully examined to establish the effect of various variables. Finally, new models are proposed based on ANNs for the prediction of crushing strength and crushing strain. The ANN models have been compared against regression-based models developed in this study.

The aim of this paper is to construct a NN model to predict the compressive strength and crushing strain of FRP-confined concrete. The NN model with one hidden layer was constructed and the training, testing and validation stages have been performed using the available test data of 272 different cylindrical FRP-confined specimens. Efforts were made to establish a methodology that would not only predict the compressive strength and crushing strain of FRP-confined concrete but provide an economic and rapid means for future experimental researchers as well. A regression based model has also been developed for the prediction of compressive strength and crushing strain of FRP-confined concrete. The test results were compared with the results predicted by neural network as well the regression models.

2. Regression models

A number of research efforts have been made on using multivariable regression models to improve the accuracy of predictions. Statistical models have the attraction that once fitted they can be used to perform predictions much more quickly than other modeling techniques and are correspondingly simpler to implement in software.

A concrete specimen has a tendency to expand under axial compression. By using FRP jacket, the lateral dilation gets confined and a state of triaxial compression is created that enhances strength and ductility of the concrete. The effect of confinement on properties of concrete was first studied by Richart et al. [46] who tested axially loaded concrete cylinders subjected to lateral fluid pressure. Based on the tests the following formula (with $\beta = 1$) to estimate the compressive strength f'_{cu} of the confined concrete was proposed which is a general form for majority of existing strength models [46]:

$$\frac{f'_{cu}}{f'_c} = 1 + \alpha\left(\frac{f_l}{f'_c}\right)^{\beta} \tag{1}$$

in which f'_{cu} and f'_c are the compressive strengths of the confined and the unconfined concrete, respectively, f_l is the lateral confining pressure, and α is the confinement effectiveness coefficient. Richart et al. [47] showed that the proposed model can also be suitable for steel-confined concrete. Fardis and Khalili [38] suggested that the above model (with $\beta = 1$) could be used for FRP-confined concrete. For application to FRP-confined concrete, f_l can be related to the thickness and strength of the FRP by:

$$f_l = 0.5\rho_j f_{ju} \tag{2}$$

where f_{ju} is the ultimate tensile strength of the FRP composite jacket and ρ_j is the confinement ratio of the FRP jacket, given by:

$$\rho_j = \frac{4t_j}{D} \tag{3}$$

where t_j is the total thickness of the FRP jacket and D is the diameter of the confined column. ACI 440 [48] adopted the model originally proposed by Mander et al. [49] for the prediction of compressive strength of concrete confined by steel jacket and later shown to be applicable for FRP-confined concrete through some modification by Spoelstra and Monti [50]. Many researchers subsequently

investigated specifically the behavior of FRP-confined concrete and consequently a considerable number of models for its compressive strength and crushing strain were developed. All of the proposed models were developed empirically by either doing regression analysis using existing test data or by a development based on the theory of plasticity with four or five parameters to be determined using available experimental data. Table 1 presents some of the important existing empirical models to predict the compressive strength and crushing strain of FRP-confined concrete since 1981.

3. Experimental data

The data used in the paper is taken from Refs. [2,4,6,8,10–37]. The data involves compression test results of 272 cylindrical FRP-confined concrete specimen with varying types of FRP composites and normal as well as high strength concrete. The data consists of five input parameters viz. diameter of cylindrical specimen; compressive strength of concrete; thickness, tensile strength and modulus of elasticity of FRP. The two output parameters are compressive strength and crushing strain of FRP-confined concrete. The database contains some subsets of two to three data with same material and geometrical parameters. These subsets cannot be averaged for the loss of variability within the subsets. Thus the data has been used in the present analysis without any modification.

The histograms of the raw variables' data used in the analysis are shown in Figs. 1–5. The minimum and maximum values of the variables are mentioned in the first and last range of variables on *X*-axis. The observations made from these figures are:

(i) Though the diameter of specimens varies from 50 and 406.4 mm (Fig. 1) but most of the data (72.4%) is for diameter close to 150 mm – normally used for determining compressive strength of concrete. The data for specimen diameter less than or equal to 70 mm and greater than 160 mm is quite low at around 5%.

(ii) The total thickness of FRP material is mostly less than 0.5 mm with 57% data for this range (Fig. 2) but the variation is from 0.089 to 7.264 mm.

(iii) There is wide range of modulus of elasticity (Fig. 3) and tensile strength of FRP (Fig. 4) because of varied materials covered in the data set which is consisting of carbon, HM-carbon, E-glass and aramid. The modulus of elasticity and tensile strength of FRP vary from 13.6 to 630 GPa and 230 to 3900 MPa respectively.

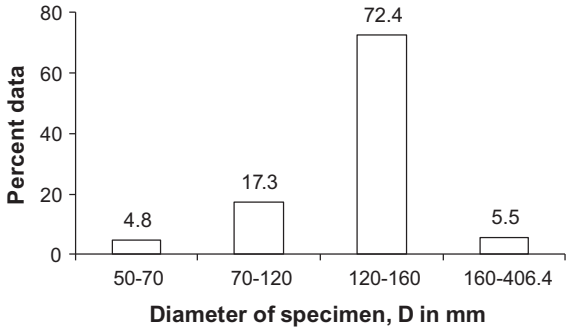

Fig. 1. Frequency distribution of the diameter of specimen.

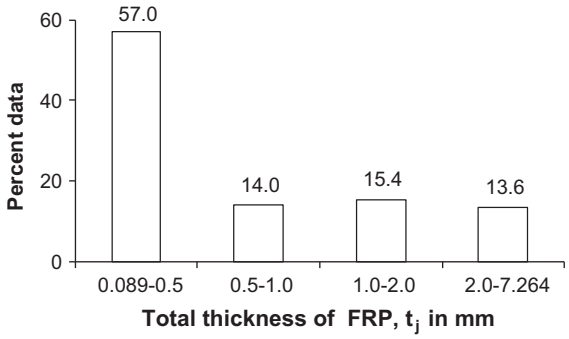

Fig. 2. Frequency distribution of the total thickness of FRP.

(iv) The data covers a wide range of compressive strength of concrete with variation from low strength concrete of 17.4 MPa to high strength concrete as strong as 169.7 MPa. Maximum data (48.2%) is for compressive strength of concrete varying from 30 to 42 MPa (Fig. 5). The data for high strength concrete (>42 MPa) is 33.4%.

4. Neural network model

Because confinement of concrete is a complex non-linear process dependent on many variables, it is a problem well suited to the artificial intelligence concept known as ANNs. Much of the current research into compressive strength and crushing strain

Table 1
Different FRP confinement models available in the literature.

Reference	Model for ultimate strength	Model for ultimate strain
Fardis and Khalili [39]	$f'_{cu} = f'_c\left[1 + 2.05\left(\frac{f_l}{f'_c}\right)\right]$	$\varepsilon_{cu} = 0.002\left[1 + 0.125\frac{E_j\rho_j}{f'_c}\right]$
Karbhari and Gao [40]	$f'_{cu} = f'_c\left[1 + 2.1\left(\frac{f_l}{f'_c}\right)^{0.87}\right]$	$\varepsilon_{cu} = 0.002\left[1 + 5\left(\frac{f_l}{f'_c}\right)\right]$
Samaan et al. [41]	$f'_{cu} = f'_c\left[1 + 6\frac{f_l^{0.7}}{f'_c}\right]$	$\varepsilon_{cu} = \frac{f'_c - 0.872f'_c - 0.371f_l - 6.258}{245.61f_c'^{0.2} + 0.3364E_j\rho_j}$
Miyauchi et al. [42]	$f'_{cu} = f'_c\left[1 + 3.5\left(\frac{f_l}{f'_c}\right)\right]$	$\varepsilon_{cu} = 0.002\left[1 + 10.6\left(\frac{f_l}{f'_c}\right)^{0.373}\right]$
Toutanji [13]	$f'_{cu} = f'_c\left[1 + 3.5\left(\frac{f_l}{f'_c}\right)^{0.85}\right]$	$\varepsilon_{cu} = \left[0.0021 + (310.57\varepsilon_{ju} + 1.90)\left(\frac{f'_{ju}}{f'_c} - 1\right)\right]$
Saafi et al. [4]	$f'_{cu} = f'_c\left[1 + 2.2\left(\frac{f_l}{f'_c}\right)^{0.84}\right]$	$\varepsilon_{cu} = 0.002\left[1 + (537\varepsilon_{ju} + 2.6)\left(\frac{f'_{ju}}{f'_c} - 1\right)\right]$
AU [37]	$f'_{cu} = f'_c\left[1 + 1.17\left(\frac{f_l}{f'_c}\right)^{0.39}\right]$	$\varepsilon_{cu} = 0.002 + 0.33\left(\frac{f_l}{f'_c}\right)^{0.77}$
Lam and Teng [7]	$f'_{cu} = f'_c\left[1 + 3.3\left(\frac{f_l}{f'_c}\right)\right]$	$\varepsilon_{cu} = 0.002\left[1.75 + 12\left(\frac{f_l}{f'_c}\right)\left(\frac{\varepsilon_{ju}}{0.002}\right)\right]^{0.45}$
Wu et al. [43]	$f'_{cu} = f'_c\left[1 + 2\left(\frac{f_l}{f'_c}\right)\right]$	$\varepsilon_{cu} = 1.786\varepsilon_{ju}\left(\frac{f_l}{f'_c}\right)^{0.66}$
Youssef et al. [9]	$f'_{cu} = f'_c\left[1 + 2.25\left(\frac{f_l}{f'_c}\right)^{1.25}\right]$	$\varepsilon_{cu} = 0.003368 + 0.259\left(\frac{f_l}{f'_c}\right)\sqrt{\varepsilon_{ju}}$
ACI 440 [48]	$f'_{cu} = f'_c\left[2.25\sqrt{1 + 7.9\frac{f_l}{f'_c}} - 2\left(\frac{f_l}{f'_c}\right) - 1.25\right]$	

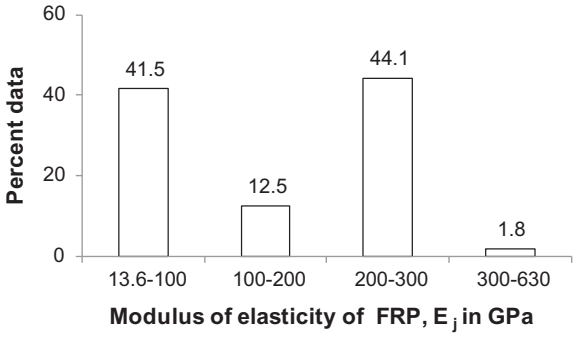

Fig. 3. Frequency distribution of the modulus of elasticity of FRP.

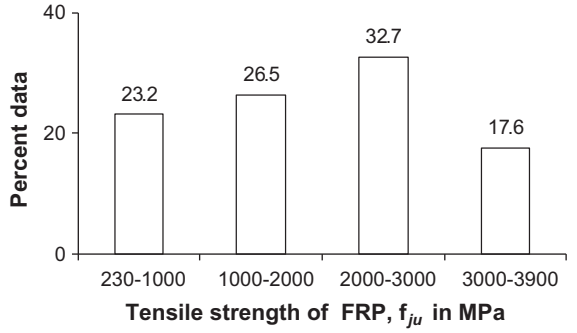

Fig. 4. Frequency distribution of the tensile strength of FRP.

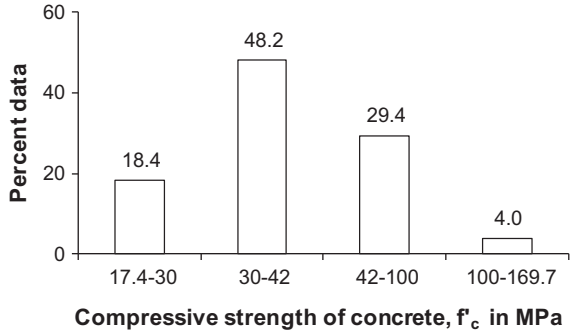

Fig. 5. Frequency distribution of the compressive strength of concrete.

prediction for unconfined concrete recognizes that neural nets are appropriate for the problem.

In the last few years, ANN technology, a sub-field of artificial intelligence, is being used to solve a wide variety of problems in civil engineering applications [51–56]. The most important property of ANN in civil engineering problems is their capability of learning directly from examples.

The manner in which the data is presented for training is the most important aspect of the neural network method. Often this can be done in more than one way; the best configuration being determined by trial-and-error. It can also be beneficial to examine the input/output patterns or data sets that the network finds difficult to learn. This enables a comparison of the performance of the neural network model for these different combinations of data. In order to map the causal relationship related to the compressive strength and ultimate strain of FRP-confined concrete, two separate input/output schemes (called Model-A1 and Model-A2) were employed, where the first takes the input of raw causal parameters while the second utilizes their non-dimensional groupings. This

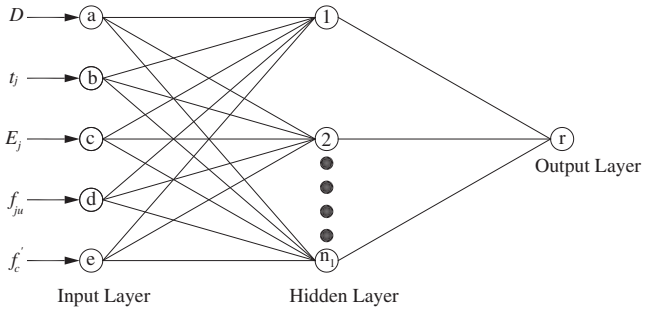

Fig. 6. Model-A1 involving use of raw variables with one hidden layer ($n_1 = 12$).

was done in order to see if the use of the grouped variables produces better results. The Model-A1 thus takes the input in the form of causative factors namely, $D, t_j, E_j, f_{ju}, f'_c$ and ε_{ju} and yields the outputs, which are the compressive strength, f'_{cu}, and crushing strain, ε_{cu}, of FRP-confined concrete:

$$\text{Model-A1}: f'_{cu} = f_1(D, t_j, E_j, f_{ju}, f'_c) \text{ and } \varepsilon_{cu} = f_2(D, t_j, E_j, f_{ju}, f'_c) \quad (4)$$

where E_j and f_{ju} are the modulus of elasticity and ultimate tensile strength of FRP jacket.

Another Model A-2 employing the dimensionless variables is given by:

$$\text{Model-A2}: \frac{f'_{cu}}{f'_c} = g_1\left(\rho_j, \frac{f_{ju}}{f'_c}, \frac{E_j}{f'_c}\right) \text{ and } \varepsilon_{cu} = g_2\left(\rho_j, \frac{f_{ju}}{f'_c}, \frac{E_j}{f'_c}\right) \quad (5)$$

The network architecture of Model-A1 employed for the prediction of compressive strength and crushing strain of FRP-confined concrete, represented by Eq. (4), is given in Fig. 6. The network architecture of Model-A2 employed for the prediction of compressive strength using single hidden layer, represented by Eq. (5) is given in Fig. 7. Whereas, the network architecture for Model-A2 with two hidden layers employed for the prediction of crushing strain is shown in Fig. 8.

Three neuron models namely, tansig, logsig and purelin, have been used in the architecture of the network with the back propagation (BP) algorithm. In the back propagation algorithm, the feed-forward (FFBP), cascade-forward (CFBP) and Elman back propagation (EBP) type networks were considered. Each input was weighted with an appropriate weight and the sum of the weighted inputs and the bias forms the input to the transfer function. The neurons employed use of the following differentiable transfer functions to generate their output:

Log-sigmoid transfer function:

$$y_j = f \cdot \left(\sum_i W_{ij}x_i + \phi_j\right) = \frac{1}{1 + e^{-\left(\sum_i W_{ij}x_i + \phi_j\right)}} \quad (6)$$

Tan-sigmoid transfer function:

$$y_j = f \cdot \left(\sum_i W_{ij}x_i + \phi_j\right) = \frac{2}{1 + e^{-2\left(\sum_i W_{ij}x_i + \phi_j\right)}} - 1 \quad (7)$$

Linear transfer function:

$$y_j = f \cdot \left(\sum_i W_{ij}x_i + \phi_j\right) = \sum_i W_{ij}x_i + \phi_j \quad (8)$$

The weight, W, and biases, ϕ, of these equations are determined in such a way as to minimize the energy function. The above transfer functions use the input x to generate layer output y. The suffix i is used for the neurons of a layer, whereas, suffix j is used for the layer number. The number of layers for models with one hidden

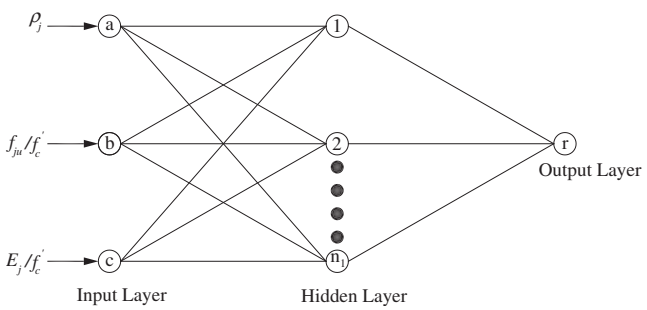

Fig. 7. Model-A2 involving use of non-dimensional variables with one hidden layer ($n_1 = 12$).

layer (Figs. 6 and 7) are two, whereas, the number of layers for the model with two hidden layers (Fig. 8) are three. The neurons of first hidden layer are generated using the input layer as the input, whereas the generation of the output layer neuron employs the preceding hidden layer as the input. The generation of neurons of second hidden layer of Fig. 8 employs first hidden layer as the input. The sigmoid transfer functions generate output between 0 and 1 or −1 and +1 as the neuron's net input goes from negative to positive infinity depending upon the use of log or tan sigmoid. When the last layer of a multilayer network has sigmoid neurons (log or tan) then the output of the network is limited to a small range, whereas, the output of linear output neurons can take on any value.

There are three phases involved in ANN modeling, viz. training, validation and testing for which separate data set is used. The current study used the data described above for the prediction of compressive strength (272 data points) and crushing strain (230 data points) of FRP-confined concrete. The training of the above two models was done using 66.67% of the data (181 data points for compressive strength and 153 for crushing strain) selected randomly. Validation and testing of the proposed models was made with the help of the remaining 33% of observations (91 data points for compressive strength and 77 for crushing strain), which were not involved in the derivation of the model. The training phase is used to adjust the weights on the neural network for which Levenberg–Marquardt non-linear least square fitting method is employed, whereas, the validation phase is used to minimize over-fitting. In the validation phase, there is no adjustment of the weights of the network with its data set; it is just to verify whether there is any increase in accuracy when a data set that has not been shown to the network before (i.e. validation data set) is also added to the training data set. The testing phase is for testing the final solution in order to confirm the actual predictive power of the network for which different error estimates have been used viz. mean percent error (MPE), mean absolute deviation percent (MAD), root mean square error (RMSE), correlation coefficient (CC), and coefficient of determination, R^2, of the linear regression line between the predicted values from the neural network model and the desired outputs. The parameter MPE gives an idea about the overall characteristic of prediction whether over or under-predicted – positive value indicates over-estimation, whereas, negative value indicates under-estimation.

The optimal architecture was determined by varying the number of hidden neurons. The optimal configuration was based upon minimizing the difference between the neural network predicted value and the desired output. In general, as the number of neurons in the layer is increased, the prediction capability of the network increases in the beginning and then becomes stationary.

The training of the neural network models was stopped when either the acceptable level of error was achieved or when the number of iterations exceeded a prescribed maximum. The neural network model configuration that minimized the MAD and RMSE and optimized the R^2 was selected as the optimum and the whole analysis was repeated several times.

5. Sensitivity analysis

Sensitivity tests were conducted to determine the relative significance of each of the independent parameters (input neurons) on the compressive strength and crushing strain of FRP-confined concrete (output) in both of the models given by Eqs. (4) and (5). In the sensitivity analysis, each input neuron was in turn eliminated from the model and its influence on the prediction of compressive strength and crushing strain of FRP-confined concrete was evaluated in terms of the MPE, MAD, RMSE, CC and R^2 criteria. The network architecture of the problem considered in the present sensitivity analysis consists of one hidden layer with 12 neurons except for crushing strain prediction model using Model A2 for which two hidden layers with 12 neurons in each layer were considered. The value of epochs was taken as 100.

5.1. Compressive strength

The results in Table 2 show that for the prediction of compressive strength using Model-A1, the variables in the order of decreasing level of sensitivity are: t_j, D, E_j, f_c' and f_{ju}. It is observed that the last parameter f_{ju} has least significant effect when taken independently. The elimination of t_j is found to have the most significant effect as it reduces the value of R^2 from 0.95 to 0.63. The available regression models (Table 1) for the prediction of compressive strength do not include E_j – third most significant parameter, whose elimination results in large reduction in the value of R^2 from 0.95 to 0.89 thus signifying the importance of its inclusion in the prediction of compressive strength of FRP-confined concrete.

Table 3 gives the results of sensitivity analysis for Model-A2. The variables in the order of decreasing level of sensitivity are:

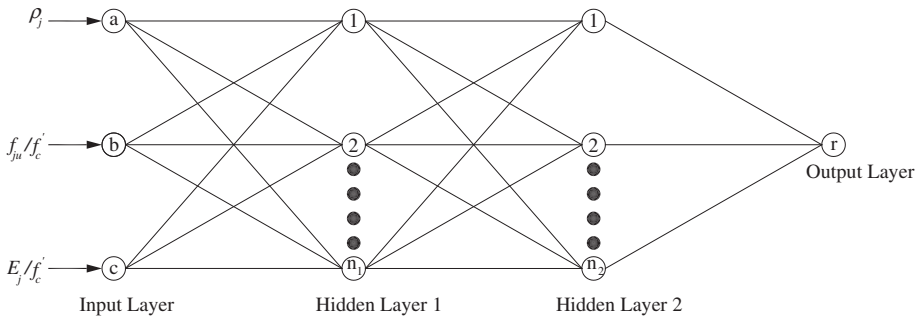

Fig. 8. Model-A2 involving use of non-dimensional variables with two hidden layers ($n_1 = n_2 = 12$).

Table 2
Sensitivity analysis of Model A-1 for the prediction of compressive strength with feed-forward back propagation for different sets of input variables.

Input variables	MPE	MAD	RMSE	CC	R^2
All (Eq. (4))	0.09	7.06	7.83	0.98	0.95
No D	3.60	11.31	13.33	0.93	0.86
No t_j	6.54	22.18	21.39	0.80	0.63
No E_j (available models)	−0.15	10.30	11.54	0.95	0.89
No f_{ju}	0.47	7.11	8.70	0.97	0.94
No f'_c	0.41	9.77	11.78	0.94	0.89

Note. MPE, mean percent error; MAD, mean absolute deviation percent; RMSE, root mean square error; CC, correlation coefficient; R^2, coefficient of determination.

Table 3
Sensitivity analysis of Model A-2 for the prediction of compressive strength with feed-forward back propagation.

Input variables	MPE	MAD	RMSE	CC	R^2
All (Eq. (5))	−0.45	8.11	0.21	0.97	0.94
No ρ_j	8.48	24.39	0.59	0.69	0.47
No f_{ju}/f'_c	1.21	9.70	0.25	0.95	0.90
No E_j/f'_c (available models)	2.77	15.95	0.43	0.85	0.72

ρ_j, E_j/f'_c and f_{ju}/f'_c. Most of the available models reported in Table 1 involve only f_l/f'_c, where f_l involves the product of ρ_j and f_{ju} thus ignoring E_j/f'_c. The drastic reduction in the value of R^2 from 0.94 to 0.72 for this case indicates that the available models incorporating only limited number of the parameters are not good enough for achieving the desired accuracy and reliability in the estimation of compressive strength of FRP-confined concrete. These findings are consistent with existing understanding of the relative importance of the various parameters on compressive strength of FRP-confined concrete. Further, ρ_j and f_{ju} are given equal weight because these are combined together in one variable f_l, whereas the sensitivity analysis indicates that the variables have significantly different levels of sensitivity. It is due to this reason that ρ_j and f_{ju} have not been combined in the present study and the same approach has also been adopted in the development a regression-based model presented latter.

5.2. Crushing strain

The results of sensitivity analysis for the prediction of crushing strain using Model-A1 are given in Table 4. It is observed from the table that the variables in the order of decreasing level of sensitivity are: t_j,f'_c,E_j,f_{ju} and D. The elimination of t_j is found to have the most significant effect as it reduces the value of R^2 from 0.90 to 0.74. Thus the variable t_j is the most significant parameter for compressive strength as well as crushing strain. The crushing strain has been taken in percent in ANN analysis.

The regression models for predicting crushing strain of FRP-confined concrete may be categorized under three groups, viz. Group-A to Group-C, on the basis of the involvement of raw variables in the model. Group-A is assumed to represent models of Karbhari and Gao [40], Miyauchi et al. [42], AU [37] and Wu et al. [43], which do not include E_j; Group-B represents Fardis and Khalili [39] model, which does not include f_{ju}; whereas, Group-C represents Samaan et al. [41], Toutanji [13], Saafi et al. [4], Lam and Teng [7] and Youssef et al. [9], which includes all raw variables. The non inclusion of f_{ju} in regression models (i.e. Group-B) show reduction in the value of R^2 from 0.90 to 0.86. Whereas, the elimination of E_j (i.e. Group-A) reduces the value of R^2 from 0.90 to 0.83.

Table 5 gives the results of sensitivity analysis for Model-A2 wherein two hidden layers each with twelve neurons are used.

Table 4
Sensitivity analysis of Model A-1 for the prediction of crushing strain with feed-forward back propagation for different sets of input variables.

Input variables	MPE	MAD	RMSE	CC	R^2
All (Eq. (4)) (Gr. C)	3.48	19.72	0.33	0.95	0.90
No D	2.41	21.62	0.36	0.94	0.89
No t_j	17.74	34.22	0.55	0.86	0.74
No E_j (Gr. A)	11.44	28.24	0.45	0.91	0.83
No f_{ju} (Gr. B)	6.32	22.80	0.40	0.93	0.86
No f'_c	14.89	36.00	0.53	0.87	0.76

Table 5
Sensitivity analysis of Model A-2 for the prediction of crushing strain with feed-forward back propagation.

Input variables	MPE	MAD	RMSE	CC	R^2
All (Eq. (5)) (Gr. C)	2.95	22.31	0.41	0.93	0.86
No ρ_j	23.40	41.70	0.59	0.84	0.71
No f_{ju}/f'_c (Gr. B)	15.74	31.16	0.53	0.88	0.76
No E_j/f'_c (Gr. A)	12.93	33.60	0.57	0.86	0.72

The variables in the order of decreasing level of sensitivity are: ρ_j, E_j/f'_c and f_{ju}/f'_c. The elimination of ρ_j is found to have the most significant effect as it reduces the value of R^2 from 0.86 to 0.71.

The above three groups viz. Groups A–C are valid even for the categorization on the basis of dimensionless variables but Samaan et al. [41] belonging to Group C may not be considered here because it is not based on the dimensionless variables. It is observed from Table 1 that Group-A does not include E_j/f'_c and Group-B does not include f_{ju}/f'_c. It is observed from the table that even the best among the groups viz. Gr. B wherein variable f_{ju}/f'_c was not included results in reduction in the value of R^2 from 0.86 to 0.76.

For compressive strength as well as crushing strain, Model-A1 using the raw variables is found to be better than Model-A2 involving dimensionless parameters. Though the difference in error parameters is small but consideration of two layers in Model-A2 when used for crushing strain makes it a bit complex; thus, for uniform approach, Model-A1 is recommended for adoption for compressive strength as well as crushing strain. The sensitivity study of both models, gives the impression that the elimination of some of the variables taken independently has only marginal influence on the resulting compressive strength of FRP-confined concrete. However, considering the limitations and uncertainties in the data and the group effect on elimination, a full-fledged network involving all input variables would be desirable.

6. Analysis and interpretation of test results

The preprocessing of the network training set was performed by normalizing the inputs and targets so that their mean is zero and standard deviations as unity. Similarly, all weights and bias values were initialized to random numbers. While the numbers of input and output nodes are fixed, the hidden nodes in the case of FFBP were subjected to trials and the one producing the most accurate results (in terms of the RMSE) was selected. The optimization of the training procedure automatically fixes the hidden nodes in the case of the CFBP. The training of these networks was stopped after reaching the minimum mean square error between the network yield and true output over all the training patterns.

The network architecture of Model-A1 employed for the prediction of compressive strength and crushing strain of FRP-confined concrete are shown earlier in Figs. 6–8. The error estimation parameters (MPE, MAD, RMSE, CC and R^2), on the basis of which the performance of a model is assessed, are already given in Tables 2–5.

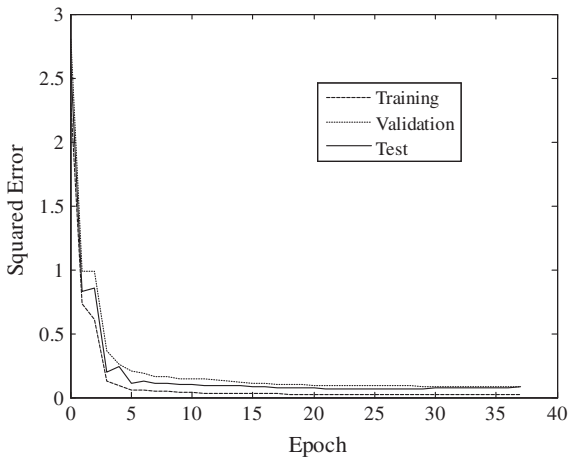

Fig. 9. Epochs versus squared error for prediction of compressive strength by back propagation using Model-A1.

6.1. Compressive strength

The training and validation for Model-A1 is shown in Fig. 9, whereas training and validation figures for other cases being similar have not been included herein. The trained values of connecting weights and bias for the two models obtained from FFBP training scheme are given in Tables 6 and 7, respectively.

A new regression model for the prediction of compressive strength of FRP confined concrete is developed:

$$f'_{cu} = f'_c\left[1 + 0.038\rho_j^{1.32}\sqrt{\frac{f_{ju}}{f'_c}}\left(\frac{E_j}{f'_c}\right)^{0.8}\left(\frac{f'_{ch}}{f'_c}\right)^{0.6}\right] \quad (9)$$

where f'_{ch} is the transitional strength of concrete demarcating normal and high strength, taken here as 42 MPa [57]. The above model further confirms the observation made in the sensitivity analysis presented above that ρ_j and f_{ju}/f'_c have different levels of sensitivity thus considering them together in parameter f_l, as done in most of the models, is not justified. The histograms of error in the prediction of the compressive strength of FRP-confined concrete for Model-A1 and Model-A2 are plotted in Fig. 10. The error in the regression model given by above Eq. (9) is also plotted in Fig. 10. The percentage error in the prediction of the concrete compressive strength for different data sets is plotted in Fig. 11 for Model-A1 whose performance is better as compared to Model-A2. The predicted value of the compressive strength of concrete has been plotted against its observed value in Figs. 12–14 for the Model-A1, proposed regression model and ACI 440 model [48], respectively.

The mean error in the proposed regression model given by Eq. (9) is 12.72%; whereas the mean errors in neural network Model-A1 and Model-A2 are only 7.06% and 8.11%, respectively. The mean error in the prediction by ACI 440 [48] is very high at 32.79% and the compressive strength is overestimated for most of the data points (Fig. 14) which is also evident from its high positive MPE value of 26.83% (Table 10). It is observed from Fig. 10 that ANN Model-A1 is slightly better than Model-A2. A comparison of ANN Model-A1 with the modified regression model, given by Eq. (9), shows that more than 94.5% of the data has error less than 15% for Model-A1 whereas, only 71.7% of the data has the same percentage of error for the proposed regression model. It is also observed from Table 10 that for about 80% of the data, the percentage error is less than 7.0% and 12.7% respectively for the two ANN models Model-A1 and Model-A2, whereas the percentage error in the regression based models for the same percentage of data is about 18.4%. This clearly indicates the supremacy of the neural network models over the regression model.

Table 6
Connection weights and biases for Model-A1 used for the prediction of compressive strength (refer to Fig. 6) (output layer bias, $\phi_2 = -0.4715$ and $R = 0.98$).

Neuron	Input–hidden layer weights, W_1					Hidden layer-output weight, W_2	Hidden layer bias, ϕ_1
	D	t_j	E_j	f_{ju}	f'_c		
1	0.6409	−1.2649	0.7899	−0.5126	0.2664	1.2213	−3.0709
2	−1.0052	−1.2199	0.4910	−0.0504	0.8316	1.0751	2.5376
3	0.5825	0.4283	−0.2359	−1.7628	−1.7607	1.5805	−0.0870
4	0.1285	−0.2656	0.2118	−1.4062	1.3161	0.9912	−0.7114
5	0.9887	−0.1970	0.6256	0.5509	−0.9922	−2.8012	−1.9259
6	−1.1374	0.3367	−1.1666	1.0688	1.8352	0.9113	−0.1329
7	−0.5814	−0.7507	0.9310	0.3597	0.2481	1.4077	−0.6819
8	−1.7538	0.5759	−0.0689	−0.5542	−0.6266	0.2143	0.3821
9	0.7777	−0.2503	−0.1289	0.4805	0.4462	1.8986	1.5160
10	0.0788	1.4177	−0.0700	−0.9084	−0.6066	1.2574	−2.6700
11	1.0540	−0.2792	−0.0749	−0.5747	−0.4378	0.3469	0.9688
12	0.2055	−0.5802	−0.3591	0.3021	0.2229	0.8170	−3.5589

Table 7
Connection weights and biases for Model-A2 used for the prediction of compressive strength (refer to Fig. 7) (output layer bias, $\phi_2 = -2.5869$ and $R = 0.97$).

Neuron	Input–hidden layer weights, W_1			Hidden layer-output weight, W_2	Hidden layer bias, ϕ_1
	ρ_j	f_{ju}/f'_c	E_j/f'_c		
1	1.7258	−1.0823	0.2819	−1.3876	−1.3134
2	0.4558	−0.4757	2.7364	−1.6919	−3.1534
3	2.5996	3.3578	−0.5815	2.6337	−2.6242
4	1.3048	−2.3271	−0.0692	0.9178	−2.2407
5	1.2933	1.6685	−2.9785	−2.1126	2.9268
6	2.3418	3.4962	−0.3467	−3.0220	−2.6499
7	−1.8502	3.2945	0.3719	−0.9687	0.2091
8	1.5212	0.9884	−3.4358	1.5081	3.4416
9	1.0410	−0.7899	−0.4957	−1.6512	1.7674
10	−1.6965	−4.4007	1.5177	0.7348	0.6545
11	2.0314	−1.1567	0.2658	2.3927	3.9775
12	−3.4991	0.5404	0.3026	−1.1090	−2.6712

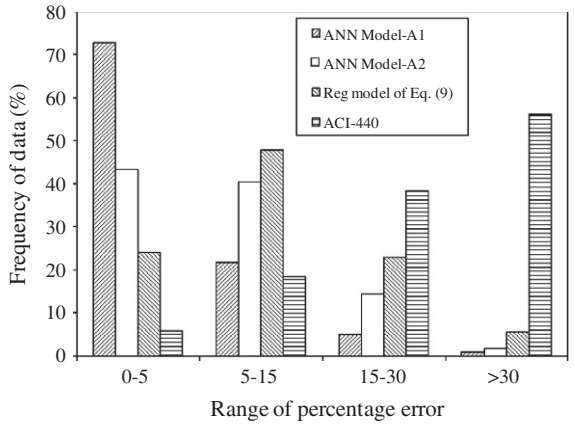

Fig. 10. Histogram of percentage error for different models of compressive strength.

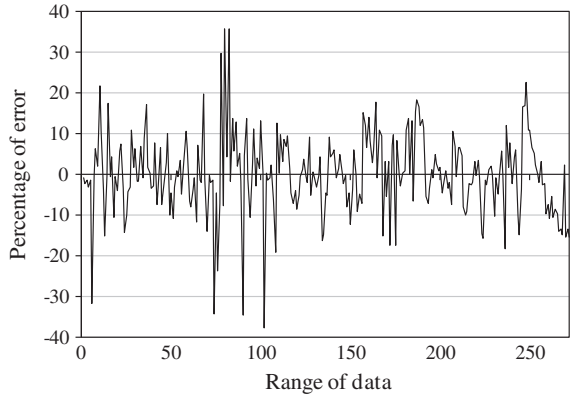

Fig. 11. Percentage error in prediction of compressive strength using Model-A1 for individual data points.

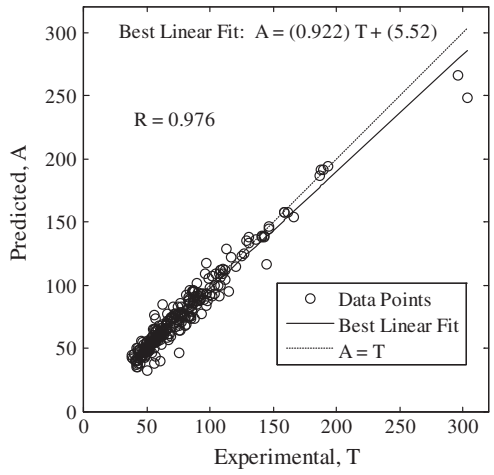

Fig. 12. Observed versus predicted compressive strength of FRP-confined concrete for Model-A1.

It is observed that the use of raw variables (i.e. Model-A1) may be more beneficial than that of the non-dimensional grouped variables as input (i.e. Model-A2), provided an appropriate training scheme is chosen. The most suitable network, FFBP Model-A2, has the highest CC = 0.98 and R^2 = 0.95; and lowest MPE = 0.09,

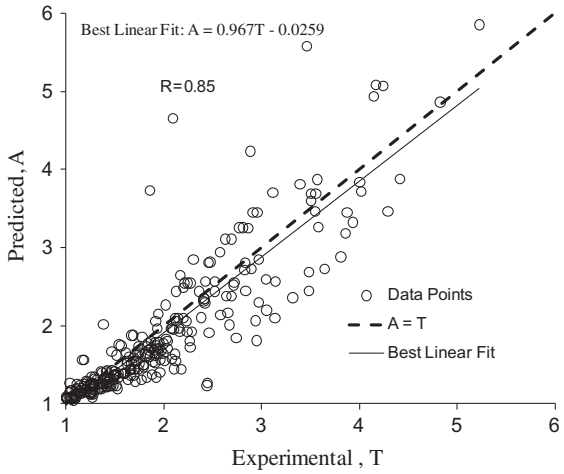

Fig. 13. Observed versus predicted compressive strength for regression model of Eq. (9).

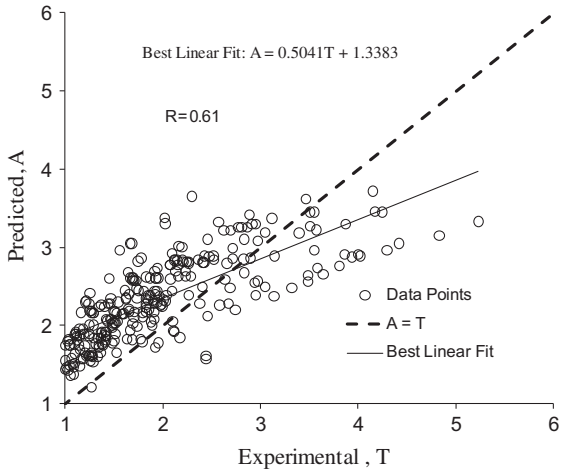

Fig. 14. Observed versus predicted compressive strength for ACI 440 [48].

MAD = 7.06 and RMSE = 7.83. All the ANN models featured small RMSE during training; however, the value was slightly higher during validation. The models showed consistently good correlation throughout the training and testing (Fig. 9).

The network configuration (FFBP Model-A1) along with corresponding weight and bias matrix given in Table 6 is thus recommended for general use in order to predict the compressive strength of FRP-confined concrete.

6.2. Crushing strain

The error estimation parameters (MPE, MAD, RMSE, CC and R^2), on the basis of which the performance of a model is assessed, are already given in Tables 4 and 5 for crushing strain.

The trained values of connecting weights and bias for Model-A1 for the prediction of crushing strain obtained from FFBP training scheme are given in Table 8. The connection weight and bias for the prediction of crushing strain using Model-A2, wherein two hidden layers with twelve neurons each are used, are given in Tables 9a and 9b.

A new regression model for the prediction of crushing strain of FRP confined concrete is developed:

$$\varepsilon_{cu} = 0.002 + 0.035\rho_j^{0.7}\left(\frac{f_{ju}}{f'_c}\right)\left(\frac{E_j}{f'_c}\right)^{0.02}\left(\frac{f'_{ch}}{f'_c}\right)^{1.3} \quad (10)$$

Table 8
Connection weights and biases for Model-A1 used for the prediction of crushing strain in percent (refer to Fig. 6) (output layer bias, $\phi_2 = -0.00619$ and $R = 0.95$).

Neuron	Input–hidden layer weights, W_1					Hidden layer-output weight, W_2	Hidden layer bias, ϕ_1
	D	t_j	E_j	f_{ju}	f'_c		
1	−2.4273	−1.7886	0.3150	0.0784	1.1914	1.8318	1.8192
2	−1.6615	−0.3102	1.1384	−0.2479	0.0662	0.5448	−0.1841
3	2.0469	0.8691	−0.6913	−0.3978	2.3242	−0.6221	−0.5340
4	0.7022	1.6985	−0.5290	2.0376	0.1049	1.3847	−1.3259
5	−2.5059	1.3147	1.2605	0.5353	−0.5972	−0.7715	2.8166
6	−0.5998	−0.6549	0.0123	0.8252	−2.0476	−0.8091	−1.0193
7	1.5121	1.3068	0.4374	−1.0890	0.2167	0.6927	−0.6104
8	−2.2440	−0.1956	−1.5241	−0.8711	1.0323	0.6338	−0.6329
9	1.7219	1.2478	−1.3179	−0.7502	−0.9534	−2.3167	−3.0031
10	−2.6217	−1.0511	0.7552	−0.6813	−0.8621	−1.6888	1.9959
11	0.2111	−2.5669	1.6236	−0.7431	−0.1703	−1.3530	2.2822
12	0.5573	−0.5218	2.4416	−1.0234	0.6897	−0.3774	−0.9207

Table 9a
Connection weights and biases for first layer of Model-A2 used for the prediction of crushing strain in percent (refer to Fig. 8).

Neuron of I hidden layer	Input-I hidden layer weights, W_1			II hidden layer-output weight, W_3	I hidden layer bias, ϕ_1	II hidden layer bias, ϕ_2
	ρ_j	f_{ju}/f'_c	E_j/f'_c			
1	−0.8181	−0.8337	−0.6303	−1.2672	2.9287	1.0600
2	3.2999	1.5260	−0.4851	−1.2182	0.6524	−1.9781
3	−1.8516	−2.4131	−1.1707	−1.2796	1.1317	−1.2888
4	0.8299	0.1194	1.7234	−0.7441	−1.8306	−0.1412
5	2.4633	−1.7445	0.0062	−1.2106	3.1169	0.8078
6	−2.3733	−1.2258	1.4393	−0.8170	−0.5896	−0.1716
7	−1.0687	0.6013	−1.3691	0.1418	2.1290	−1.0842
8	−1.9369	1.0473	−0.3414	−1.3588	0.9908	0.3103
9	0.1015	−1.8694	2.7420	0.7388	0.2943	−1.0944
10	1.8157	0.4799	−3.4563	2.2523	3.0967	1.1462
11	0.2802	1.7432	−0.2572	−2.6518	−1.7823	1.2848
12	1.2239	1.6394	−1.1316	−0.5002	−1.7065	2.1447

Table 9b
Connection weights and biases for second layer of Model-A2 used for the prediction crushing strain in percent (refer to Fig. 8) (output layer bias, $\phi_3 = -0.0264$ and $R = 0.93$).

Neuron of II hidden layer	Weight for neuron of I–II hidden layer, W_2											
	Neuron of I hidden layer											
	1	2	3	4	5	6	7	8	9	10	11	12
1	−0.823	0.494	−1.064	0.749	0.791	−0.864	−0.895	0.460	0.884	−1.389	1.280	1.249
2	−0.173	0.415	−1.437	−0.365	0.343	1.964	1.213	0.719	1.687	−0.329	0.583	−0.751
3	0.614	−1.857	0.250	−0.173	0.006	−1.140	−1.468	0.516	−0.878	1.144	0.008	0.205
4	1.368	−0.336	1.062	−1.123	−0.079	−1.328	1.470	0.766	0.610	−0.333	0.099	0.536
5	0.280	−0.352	0.915	−1.068	−0.302	0.757	1.221	0.698	−0.974	−0.106	−0.498	0.874
6	−0.959	1.323	−0.189	1.279	0.210	−0.127	0.195	0.072	−0.259	0.205	0.715	−0.621
7	−1.552	−0.066	0.305	0.752	0.830	1.144	−0.443	0.162	−1.679	1.140	0.283	0.830
8	0.481	0.696	0.297	0.394	−0.383	−1.113	−0.760	−0.973	1.163	0.076	0.474	−0.094
9	−1.238	0.738	−0.900	0.106	0.405	−0.038	−0.571	0.650	−0.410	0.059	0.626	0.201
10	0.237	1.484	−0.766	−0.479	−1.412	0.735	0.095	−1.138	1.164	0.937	0.419	−0.233
11	0.113	0.902	−1.777	0.340	1.165	0.395	0.362	−0.420	−0.537	−2.493	0.409	−2.079
12	0.807	−0.855	−0.286	0.268	0.080	−0.262	0.530	−0.478	−0.491	−0.058	−1.101	−0.140

The above model also shows that ρ_j is the most significant parameter as observed earlier in the sensitivity analysis. The histograms of error in the prediction of the crushing strain of FRP-confined concrete for Model-A1 and Model-A2 are plotted in Fig. 15. The error in the regression model given by Eq. (10) is also plotted in Fig. 15. The percentage error in the prediction of the crushing strain for different data sets is plotted in Fig. 16 for Model-A1 which is found to be better than Model-A2. The predicted value of the crushing strain of FRP-confined concrete has been plotted against its observed value in Figs. 17 and 18 for the Model-A1 and regression model respectively. The error estimates for the two ANN models and proposed regression models for crushing strength and crushing strain are summarized in Table 10. The error estimates for the prediction of compressive strength using ACI 440 [48] are also given in the table. Besides the five error estimates considered above for the ANN models, two additional estimates (viz. percent data for error within 15% range and percentage of error enveloping 80% of the data) for judging the performance of models have been considered. It may be noted here that the RMSE of ANN Model-A1 for compressive strength may not be compared with other models because of the difference in the form of output which is dimensioned for Model-A1, whereas it is non-dimensional in other models.

The mean error in the modified regression model given by Eq. (10) is 29.87%; whereas the mean errors in neural network Model-A1 and Model-A2 are only 19.72% and 22.31%, respectively. It is observed from Fig. 15 that ANN Model-A1 is slightly better than Model-A2. A comparison of ANN Model-A1 with the modified regression model, given by Eq. (10), shows that more than 57.8% of the data has error less than 15% for Model-A1 whereas, only 33.9%

Table 10
Error estimates for different models.

Parameter for error estimate	Compressive strength				Ultimate compressive strain		
	ANN Model-A1	ANN Model-A2	Regression model of Eq. (9)	ACI 440 [48]	ANN Model- A1	ANN Model-A2	Regression model of Eq. (10)
Mean percent error (MPE)	0.09	−0.45	4.30	26.83	3.48	2.95	4.50
Mean absolute deviation in percent (MAD)	7.06	8.11	12.72	32.79	19.72	22.31	29.87
Root mean square error (RMSE)	7.83	0.21	0.42	0.64	0.33	0.41	0.33
Coefficient of correlation (CC)	0.98	0.97	0.85	0.61	0.95	0.93	0.90
Coefficient of determination, R^2	0.95	0.94	0.73	0.37	0.90	0.86	0.81
Percent data for error within 15%	94.5	83.8	71.7	23.9	57.8	55.2	33.9
Percentage error enveloping 80% data	7.0	12.7	18.4	36.9	29.9	32.4	42.4

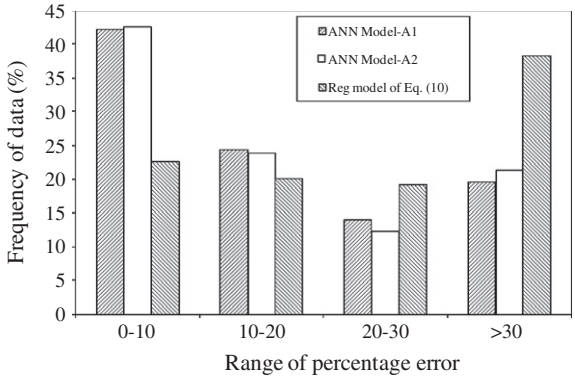

Fig. 15. Histogram of percentage error for different models of crushing strain.

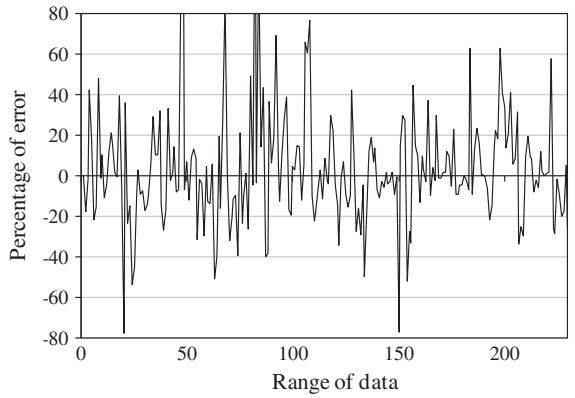

Fig. 16. Percentage error in prediction of crushing strain in percent by Model-A1 for individual data points.

of the data has the same percentage of error for the regression model (Fig. 15). It was also observed from Table 10 that for about 80% of the data, the percentage error is less than 29.9% and 32.4% respectively for the two ANN models Model-A1 and Model-A2 respectively, whereas the percentage error in the regression based models for the same percentage of data is about 42.4%. This clearly indicates the supremacy of the neural network models over the regression model.

It is observed that the use of raw variables (i.e. Model-A1) may be more beneficial than that of the non-dimensional grouped variables as input (i.e. Model-A2), provided an appropriate training scheme is chosen. The most suitable network, FFBP Model-A1, has the highest CC = 0.95 and R^2 = 0.90; and lowest MPE = 3.48, MAD = 19.72 and RMSE = 0.33. All the ANN models featured small RMSE during training; however, the value was slightly higher during validation. The models showed consistently good correlation throughout the training and testing.

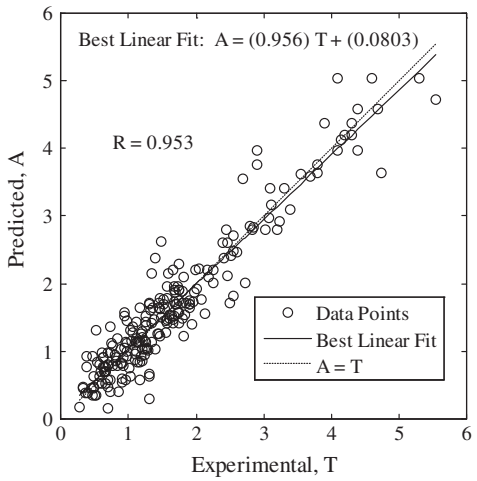

Fig. 17. Observed versus predicted ultimate strain in percent using Model-A1.

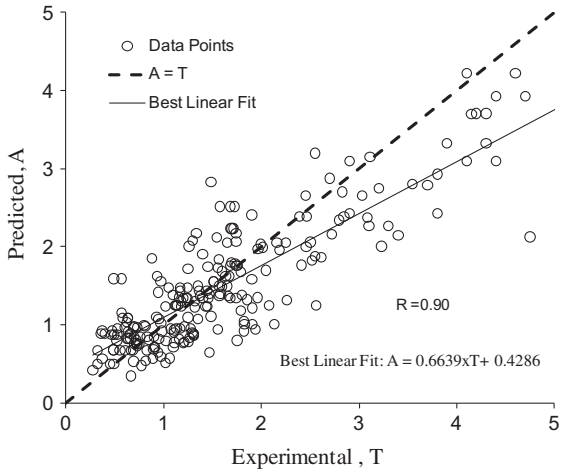

Fig. 18. Observed versus predicted ultimate strain in percent for regression model of Eq. (10).

The network configuration (FFBP Model-A1) along with corresponding weight and bias matrix given in Table 8 is thus recommended for general use in order to predict the crushing strain of FRP-confined concrete.

7. Conclusions

A generalized model for predicting the compressive strength and crushing strain of FRP-confined concrete using neural network

has been developed. The network predictions were generally more satisfactory than those given by traditional regression equations and the one developed in this study because of low errors and high correlation coefficients. The compressive strength as well as the crushing strain predictions based on raw data ($D, t_j, E_j, f_{ju}, f'_c$) were better than those based on the dimensionless grouped variables. The neural network with one hidden layer was selected as the optimum network to predict the compressive strength of as well as the crushing strain of FRP-confined concrete. Thus network configuration of Model-A1 with FFBP is recommended for general use in order to predict the compressive strength as well as crushing strain of FRP-confined concrete. On the basis of sensitivity analysis for the prediction of compressive strength, it is observed that the thickness of FRP jacket, t_j, diameter of cylindrical specimen, D, modulus of elasticity, E_j, and compressive strength of concrete, f'_c are the four most significant parameters for the prediction of compressive strength as well as the crushing strain of FRP-confined concrete.

From the study of sensitivity of Model-A1 and Model-A2 and considering the variability in the outcome resulting from application of different analytical schemes, it is felt that the network which requires all input quantities may be followed for generality. The neural network model is far better than the regression models in the prediction of the compressive strength and crushing strain of FRP-confined concrete.

Acknowledgements

The authors gratefully acknowledge the support provided by the Specialty Units for Safety and Preservation of Structures and the MMB Chair of Research and Studies in Strengthening and Rehabilitation of Structures, Department of Civil Engineering, King Saud University.

References

[1] Saadatmanesh H, Ehsani MR, Li MW. Strength and ductility of concrete columns externally reinforced with fiber composite straps. ACI Struct J 1994;91(4):434–47.
[2] Demers M, Neale KW. Strengthening of concrete columns with unidirectional composite sheets. In: Mufti AA, Bakht B, Jaeger LG, editors. Development is short and medium span bridge engineering' 94. Proceedings of the fourth international conference on short and medium bridges. Montreal: Canadian Society for Civil Engineering; 1994. p. 895–905.
[3] Toutanji H, Balagurce P. Durability characteristics of concrete columns wrapped with FRP two sheets. J Mater Civ Eng 1998;5:52–7.
[4] Saafi M, Toutanji HA, Li Z. Behavior of concrete columns confined with fiber reinforced polymer tubes. ACI Mater J 1999;96(4):500–9.
[5] Parvin A, Jamwal AS. Effects of wrap thickness and ply configuration on composite-confined concrete cylinders. Compos Struct 2005;67(4):437–42.
[6] Berthet JF, Ferrier E, Hamelin P. Compressive behavior of concrete externally confined by composite jackets. Part A: experimental study. Construct Build Mater 2005;19(3):223–32.
[7] Lam L, Teng JG. Design-oriented stress–strain model for FRP confined concrete. Construct Build Mater 2003;17(6–7):471–89.
[8] Almusallam TH. Behavior of normal and high-strength concrete cylinders confined with E-glass/epoxy composite laminates. J Compos: Part B 2007;38:629–39.
[9] Youssef MN, Feng MQ, Mosallam AS. Stress–strain model for concrete confined by FRP composites. J Compos: Part B 2007;38:614–28.
[10] Youssef MN. Stress–strain model for concrete confined by FRP composites. Ph.D. dissertation, University of California, Irvine; March 2003.
[11] Harmon TG, Slattery KT. Advanced composite confinement of concrete. In: Neale KW, Labossiere P, editors. Proceedings of the first international conference on advanced composite materials in bridge and structures. Sherbocke, Canada: Canadian Society for Civil Engineering; 1992. p. 299–306.
[12] Kono S, Inazumi M, Kaku T. Evaluation of confining effects of CFRP sheets on reinforced concrete members. In: Proceedings of the second international conference on composites in infrastructure ICCI'98, Tucson, Arizona, 5–7 January; 1998. p. 343–55.
[13] Toutanji HA. Stress–strain characteristics of concrete columns externally confined with advanced fiber composite sheets. ACI Mater J 1999(May–June):397–404.
[14] Micelli F, Myers JJ, Murthy S. Effect of environmental cycles on concrete cylinders confined with FRP. In: Proceedings of CCC2001 international conference on composites in construction, Porto, Portugal; 2001.
[15] Lin CT, Li YF. An effective peak stress formula for concrete confined with carbon fiber reinforced plastics. Can J Civil Eng 2003;30:882–9.
[16] Watanable K, Nakamura H, Honda T, Toyoshima M, Iso M, Fujimaki T, et al. Confinement effect of FRP sheet on strength and ductility of concrete cylinders under uniaxial compression. In: Non-metallic (FRP) reinforcement for concrete structures, proceedings of the third international symposium, vol. 1. Sapporo, Japan: Japan Concrete Institute; 1997. p. 233–40.
[17] Matthys S, Taerwe L, Audenaert K. Tests on axially loaded concrete columns confined by fiber reinforced polymer sheet wrapping. In: Dolan CW, Rizkalla SH, Nanni SH, editors. Proceedings of the fourth international symposium on fiber reinforced polymer reinforcement for reinforced concrete structures, SP-188. Farmington, Michigan, USA: American Concrete Institute; 1999. p. 217–29.
[18] Kshirsagar S, Lopez-Anido RA, Gupta RK. Environmental aging of fiber-reinforced polymer-wrapped concrete cylinders. ACI Mater J 2000;97(6):703–12.
[19] Rochette P, Labossiere P. Axial testing of rectangular column models confined with composites. J Compos Constr, ASCE 2000;4(3):129–36.
[20] Xiao Y, Wu H. Compressive behavior of concrete confined by carbon fiber composite jackets. J Mater Civ Eng ASCE 2000;12(2):139–46.
[21] De Lorenzis L, Micelli F, La Tegola A. Influence of specimen size and resin type on the behavior of FRP-confined concrete cylinders. In: Shenoi RA, Moy SSJ, Hollaway LC, editors. Advanced polymer composites for structural applications in construction, proceedings of the first international conference. London, UK: Thomas Telford; 2002. p. 231–9.
[22] Picher F, Rochette P, Labossiere P. Confinement of concrete cylinders with CFRP. In: Saadatmanesh H, Ehsani MR, editors. Proceedings of the first international conference on composites for infrastructures. Tucson, Arizona, USA: University of Arizona; 1996. p. 829–41.
[23] Purba BK, Mufti AA. Investigation of the behavior of circular concrete columns reinforced with carbon fiber reinforced polymer (CFRP) jackets. Can J Civ Eng 1999;26:590–6.
[24] Aire C, Gettu R, Casas JR. Study of the compressive behavior of concrete confined by fiber reinforced composites. In: Figueiras J, Juvandes L, Faria R, Marques AT, Ferreira A, Barros J, et al., editors. Composites in constructions, proceedings of the international conference. Lisse, The Netherlands: A.A. Balkema Publishers; 2001. p. 239–43.
[25] Shehata IAEM, Carneiro LAV, Shehata LCD. Strength of short concrete columns confined with CFRP sheets. Mater Struct 2002;35(1):50–8.
[26] Campione G, Miraglia N, Scibilia N. Comportamento in compression di elementi in calcestruzzo armato a sezione quadrata e circolare rinforzati con FRP. Ingegneria Sismica, vol. 2; 2001 [in Italian].
[27] Arduini M, Di Tommaso A, Mantegazza G. Compositi per la riabilitazione strutturale. Atti delle Giornate AICAP 97 1997;1:29–240 [in Italian].
[28] Bortolotti L, Lai S, Carta S, Cireddu D. Comportamento a carico assiale di conglomerati ad alta resistenza confinati con tessuto di fibra di carbonio. Atti delle Giornate AICAP 99 1999;1:5–14 [in Italian].
[29] Demers M, Neale WK. Confinement of reinforced concrete columns with fibre-reinforced composite sheets – an experimental study. Can J Civ Eng 1999;26:226–41.
[30] Al-Salloum YA, Almusallam TH, Elsanadedy HM, Abadel AA. Effect of specimen size on the strength of FRP-confined concrete. In: ICPIC 2010 – 13th international congress on polymers in concrete; November 2009.
[31] Lam L, Teng JG. Ultimate condition of fiber reinforced polymer-confined concrete. J Compos Constr, ASCE 2004;8(6):539–48.
[32] Lam L, Teng JG, Cheung CH, Xiao Y. FRP-confined concrete under axial cyclic compression. Cem Concr Compos 2006;28(10):949–58.
[33] Teng JG, Yu T, Wong YL, Dong SL. Hybrid FRP-concrete–steel tubular columns: concept and behaviour. Construct Build Mater 2007;21(4):846–54.
[34] Jiang T, Teng JG. Analysis-oriented stress–strain models for FRP–confined concrete. Eng Struct 2007;29:2968–86.
[35] Shahawy M, Mirmiran A, Beitelman T. Tests and modeling of carbon-wrapped concrete column. J Compos: Part B 2000;31:471–80.
[36] Mirmiran A, Zagers K, Yuan W. Nonlinear finite element modeling of concrete confined by fiber composites. J Finite Elem Anal Des 2000;35:79–96.
[37] AU C. Behavior of FRP-confined concrete. MS thesis, Massachusetts Institute of Technology; May 2001.
[38] Fardis MN, Khalili H. Concrete encased in fiber glass reinforced plastic. ACI Struct J 1981;78:440–5.
[39] Fardis MN, Khalili H. FRP-encased concrete as a structural material. Mag Concr Res 1982;34(121):191–202.
[40] Karbhari VM, Gao Y. Composite jacketed concrete under uniaxial compression–verification of simple design equations. J Mater Civ Eng 1997;9(4):185–93.
[41] Samaan M, Mirmiran A, Shahawy M. Model of concrete confined fiber composite. J Struct Eng, ASCE 1998;124(9):1025–31.
[42] Miyauchi K, Inoue S, Kuroda T, Kobayashi A. Strengthening effect of concrete columns with carbon fibre sheet. Trans Jpn Concr Inst 1999;21:143–50.
[43] Wu G, Lu ZT, Wu ZS. Strength and ductility of concrete cylinders confined with FRP composites. Construct Build Mater 2006;20:134–48.
[44] Lignola GP, Prota A, Manfredi G, Cosenza E. Evaluation of effective ultimate strain of FRP confinement jackets applied on circular RC columns. In: FRPRCS-9

9th international symposium on fiber reinforced polymer reinforcement for concrete structures, Sydney, Australia; 13–15 July 2009.
[45] Ludovico MD, Lignola GP, Prota A, Manfredi G, Cosenza E. Effective strains on frp confinement of concrete members: experimental–theoretical comparisons. In: FRPRCS-9 9th international symposium on fiber reinforced polymer reinforcement for concrete structures, Sydney, Australia; 13–15 July 2009.
[46] Richart FE, Brandtzaeg A, Brown RL. A study of the failure of concrete under combined compressive stresses, Urbana, Illinois, USA. Bulletin No. 185, University of Illinois, Engineering Experimental Station; 1928.
[47] Richart FE, Brandtzaeg A, Brown RL. The failure of plain and spirally reinforced concrete in compression, Urbana, Illinois, USA. Bulletin No. 185, University of Illinois, Engineering Experimental Station; 1929. p. 1929.
[48] ACI 440. Guide for the design and construction of externally bonded FRP systems for strengthening concrete structures. Detroit, Mich.: American Concrete Institute; 2002.
[49] Mander JB, Priestley MJN, Park R. Theoretical stress–strain model for confined concrete. J Struct Eng, ASCE 1988;114(8):1804–26.
[50] Spoelstra MR, Monti G. FRP-confined concrete model. J Compos Construct, ASCE 1999;3(3):143–50.
[51] Bai J, Wild S, Ware JA, Sabir BB. Using neural networks to predict workability of concrete incorporating metakaolin and fly ash. Adv Eng Softw 2003;34(11–12):663–9.
[52] Topcu IB, Saridemir M. Prediction of properties of waste AAC aggregate concrete using artificial neural network. Comput Mater Sci 2007;41(1):117–25.
[53] Topcu IB, Saridemir M. Prediction of compressive strength of concrete containing fly ash using artificial neural network and fuzzy logic. Comput Mater Sci 2008;41:305–11.
[54] Topcu IB, Saridemir M. Prediction of rubberized concrete properties using artificial neural network and fuzzy logic. Construct Build Mater 2008;22:532–40.
[55] Çanakci H, Pala M. Tensile strength of basalt from a neural network. Eng Geol 2007;94(1–2):10–8.
[56] Adhikary BB, Mutsuyoshi H. Prediction of shear strength of steel fiber RC beams using neural networks. Construct Build Mater 2006;20:801–11.
[57] ACI 318-08. Building code requirements for structural concrete and commentary. Detroit, Mich.: American Concrete Institute; 2008.